ARTICLE

Photoelectrochemical oxidation of organic substrates in organic media

Tengfei Li[1], Takahito Kasahara[1], Jingfu He[1], Kevan E. Dettelbach[1], Glenn M. Sammis[1] & Curtis P. Berlinguette [1,2,3]

There is a global effort to convert sunlight into fuels by photoelectrochemically splitting water to form hydrogen fuels, but the dioxygen byproduct bears little economic value. This raises the important question of whether higher value commodities can be produced instead of dioxygen. We report here photoelectrochemistry at a $BiVO_4$ photoanode involving the oxidation of substrates in organic media. The use of MeCN instead of water enables a broader set of chemical transformations to be performed (e.g., alcohol oxidation and C-H activation/oxidation), while suppressing photocorrosion of $BiVO_4$ that otherwise occurs readily in water, and sunlight reduces the electrical energy required to drive organic transformations by 60%. These collective results demonstrate the utility of using photoelectrochemical cells to mediate organic transformations that otherwise require expensive and toxic reagents or catalysts.

[1] Department of Chemistry, The University of British Columbia, 2036 Main Mall, Vancouver, Canada BC V6T 1Z1. [2] Department of Chemical & Biological Engineering, The University of British Columbia, 2036 Main Mall, Vancouver, Canada BC V6T 1Z1. [3] Present address: Stewart Blusson Quantum Matter Institute and Department of Chemical ‖ Biological Engineering, The University of British Columbia, 2036 Main Mall, Vancouver, Canada BC V6T 1Z1. Correspondence and requests for materials should be addressed to G.M.S. (email: gsammis@chem.ubc.ca) or to C.P.B. (email: cberling@chem.ubc.ca)

nterfacial photoelectrochemistry (PEC) at a semiconductor-
liquid junction enables the direct conversion of light
into chemical energy[1–3]. The highly energetic electrons and
holes that are created through the absorption of visible light
by semiconducting electrodes are capable of driving the energe-
tically demanding conversion of water into oxygen and hydrogen
fuels[4–6]. While there has been a large global effort to reduce the
relatively large energy losses associated with producing oxygen at
the anode, strikingly few photoanodes are known to be capable of
both absorbing incident sunlight and mediating efficient and
sustained water oxidation catalysis[7–11].

The technical challenges of using a photoanode to form
dioxygen that has little economic value provides the imperative
to explore alternative reactions that generate higher value
products with lower energy input. Choi and coworkers recently
demonstrated that the photoelectrochemical oxidation of
5-hydroxymethylfurfural into 2,5-furandicarboxylic acid could be
realized with a BiVO$_4$ photoanode in the presence of a redox
mediator[12]. A key challenge of this distinctive approach, however,
is that the aqueous medium limits the scope of chemistry
available and induces high rates of BiVO$_4$ photocorrosion[13, 14].
While photocorrosion in H$_2$O can be suppressed by a protective
(electrocatalytic) layer (e.g., CoO$_x$, NiO$_x$, and FeO$_x$)[14–16], these
layers tend to suppress the oxidation of organic compounds in
favor of competitive oxygen evolution[12, 17].

We therefore set out to explore conditions where the
photoelectrochemically-driven oxidation of organic compounds
in non-aqueous media could be achieved. Two classes of well
known organic transformations were chosen to test this concept:
alcohol oxidation and the more challenging C–H functionaliza-
tion/oxidation (Fig. 1). The oxidation of alcohols can be readily
achieved using chemical oxidizing agents that include transition
metals, hypervalent iodine reagents, and activated sulfur trans-
formations[18, 19]. Some of these alcohol oxidation reactions have
also been conducted using an electrode[20–22], photo-oxidized dyes
immobilized on TiO$_2$[23], and, as mentioned above, a photo-
anode[12]. The activation and subsequent functionalization of C–H
bonds is a greater challenge[24]. The respective transformation of
olefin and alkylbenzene compounds into α,β-unsaturated and aryl
ketones, for example, usually requires toxic reagents (e.g., CrO$_3$
and SeO$_2$) and/or expensive metal catalysts (e.g., Rh and Pd)[24, 25],
but allylic C–H oxidation can also be driven electrochemically at a
carbon electrode[26, 27]. Note that the electrochemical (EC) study
by Baran and coworkers was performed in non-aqueous media,
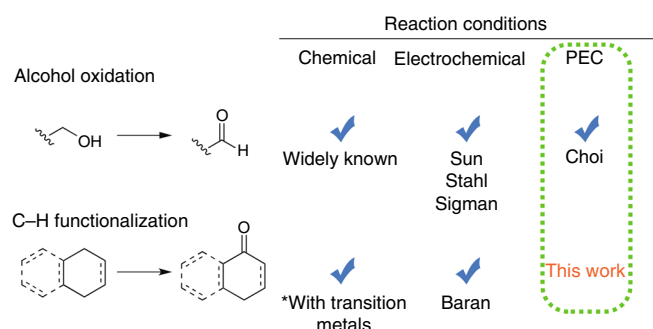thereby enabling them to oxidize a large set of substrates with
reasonable yields (40–90%)[26].

We report here the use of a PEC cell to mediate organic
oxidation reactions using a photoanode immersed in organic
media. The photoelectrochemical oxidation of benzyl alcohol,
cyclohexene, and tetralin into their corresponding carbonyl
compounds were demonstrated in a PEC cell containing a BiVO$_4$
photoanode immersed in MeCN containing appropriate reaction
mediators (e.g., electrolyte, base, and electron transfer reagent).
Product formation can be achieved using a 60% reduction in the
applied voltage compared to a purely EC oxidation. Furthermore,
no significant degradation of the photoanode was observed.

Results

**Photoelectrochemical stability of BiVO$_4$ in non-aqueous
media.** The BiVO$_4$ photoanodes used in this study were synthe-
sized in accordance with documented procedures[28]. Appropriate
stoichiometric amounts of bismuth nitrate hexahydrate
and vanadyl acetylacetonate precursors dissolved in a solution
of acetic acid and acetylacetone were spin-coated onto fluorine-
doped tin oxide (FTO), annealed at 500 °C, and then subjected
to ultraviolet (UV) irradiation (λ_{max} ~185 and 254 nm, flux
~10 mW cm^{-2}) in air for 20 h. This UV radiation step
renders higher activity for aqueous PEC[28, 29]. The UV-Vis
absorption spectra, surface morphology, and powder X-ray
diffractograms of the films are consistent with previous descrip-
tions of BiVO$_4$ prepared by this protocol (Fig. 2, Supplementary
Figs. 1 and 2)[10, 28].

The photoelectrochemical stability of BiVO$_4$ in aqueous and
non-aqueous media was tested by measuring the absorptivity
changes before and after 96 h of illumination under an applied
potential. The photoanodes were immersed in 25 mL H$_2$O
containing 0.1 M NaHCO$_3$ or 25 mL MeCN with 0.1 M LiClO$_4$
and exposed to simulated AM1.5 G sunlight for 24 h and an
applied potential of 0.1 or 1.6 V, respectively (all potentials
reported herein are referenced against Ag/AgCl). The anodes
were then left in solution in the dark for 24 h at open-circuit prior
to a subsequent 24 h of PEC electrolysis at these same potentials.
UV-Vis absorption spectra of the photoanodes recorded after
four successive cycles in H$_2$O (i.e. ~96 h of cumulative exposure
to PEC conditions) showed a much more significant reduction in
intensity over the 400–600 nm range than those in MeCN
(Fig. 2a). This reduced absorptivity is consistent with a decrease
in BiVO$_4$ film thickness, while the nominal changes in
absorptivity of the photoanode in MeCN after PEC indicate
insignificant photocorrosion. The solvent-dictated differences in
photoanode stability were corroborated by photocurrent
measurements of BiVO$_4$ before and after PEC in both solvents
(Fig. 2b): The anode tested in H$_2$O exhibited a striking drop in
photocurrent after 96 h of PEC electrolysis, whereas the
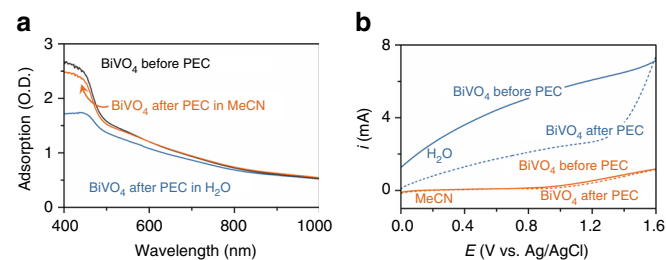photocurrents recorded in MeCN did not change. The

Fig. 1 Summary of reaction conditions for alcohol oxidation and C–H
functionalization. Three types of reaction conditions (chemical oxidation,
EC oxidation at an electrode[20–22, 26], and photoelectrochemical
oxidation[12]) that have been used for alcohol oxidation and C–H
functionalization are shown. We report here C–H functionalization and
oxidation by PEC

Fig. 2 Demonstration of lower BiVO$_4$ photocorrosion in MeCN than in H$_2$O.
a UV-Vis absorption spectra of BiVO$_4$ photoanodes before (*black*) and after
96 h of PEC in H$_2$O (*blue*) or MeCN (*orange*). **b** Photocurrents of BiVO$_4$
photoanodes before (*solid line*) and after (*dashed line*) 96 h of PEC
electrolysis in H$_2$O (*blue*) or MeCN (*orange*)

photoanodes tested in MeCN with increasing amounts of water also showed an increasing propensity for photocorrosion (Supplementary Table 1). The accelerated photocorrosion of $BiVO_4$ in H_2O was confirmed by scanning electron microscope (SEM) images of photoanodes before and after 96 h of PEC. Full coverage of FTO by spherical grains of $BiVO_4$ (Supplementary Fig. 2) are retained for the photoanodes subjected to 96 h of PEC electrolysis in MeCN, with visible FTO providing evidence for less uniform coverage in films exposed to aqueous PEC. This morphology change during PEC electrolysis in H_2O is widely known[14, 16]. While organic solvents increase the resistance of the PEC cell (~10–20 Ω with MeCN *c.f.* <10 Ω using water), merely ~30 mV in additional voltage is required at the low currents (~3 mA) relevant to this study. This additional voltage represents a modest energy penalty for the much higher photoanode stability.

Photoelectrochemical alcohol oxidation. Having validated the photostability of $BiVO_4$ in MeCN, we tested the oxidation of organic substrates using a PEC cell. All experiments were carried out in MeCN containing $LiClO_4$ electrolyte. Other organic solvents (e.g. acetone and CH_3NO_2) and electrolytes (e.g. Bu_4NClO_4 and Bu_4NPF_6) were tested but did not yield any discernible benefit in photocurrent or product yield. MeCN was utilized as the solvent because because the boiling point (82 °C) is sufficiently high to minimize evaporation during electrolysis and sufficiently low to circumvent interfering with the gas chromatography-mass spectrometry (GC-MS) analysis. $LiClO_4$ was selected on the basis of it being a cheap electrolyte that is soluble in organic media.

Linear sweep voltammetry (LSV) was measured under AM1.5 G light prior to performing PEC electrolysis (Fig. 3). Photocurrent profiles recorded on the $BiVO_4$ working electrode in 25 mL of MeCN containing 0.1 M $LiClO_4$, a glassy carbon counter electrode (CE), and an Ag/AgCl reference electrode (RE), generated nominal current below ca. 1 V. For each of the organic reactions in this study, pyridine served as the requisite base to accommodate deprotonation of *N*-hydroxysuccinimide (NHS), a soluble, transparent, and electrochemically active species that proved effective at mediating hole transfer from the electrode to the organic substrate. Baseline photocurrent profiles were measured prior to addition of 0.5 mmol of substrate: 4 equiv. pyridine (162 μL; 2 mmol) caused a small but detectable change in LSV photocurrent below 1 V (Fig. 3), while the subsequent addition of 40 mol% NHS (23 mg; 0.2 mmol) caused a more dramatic rise in current. The shoulder at 0.8 V (indicated by the vertical dashed lines in Fig. 3) is assigned to the oxidation of NHS^- to electrochemically-active $NHS\bullet$[30]. All organic oxidation reactions in this report were therefore carried out under an applied voltage of 0.8 V (denoted V_{app}), which is sufficiently low to avoid solvent and pyridine oxidation yet sufficiently positive to generate the $NHS\bullet$ species required for oxidation of the organic substrates. The $BiVO_4$ photoanodes after 96 h of PEC with substrate exhibit minor differences in absorptivity and LSV photocurrents consistent with negligible photocorrosion (Supplementary Figs. 2 and 3), but not to a degree that compromises these experiments.

The facile oxidation of benzyl alcohol to benzaldehyde was selected as a proof-of-concept experiment because alcohol oxidation was previously shown to proceed at a $BiVO_4$ photoanode in H_2O[12]. The photocurrent increased after the addition of 0.5 mmol benzyl alcohol to the PEC cell described above (Fig. 3a). This increase is assumed to be due to the consumption of $NHS\bullet$ (which oxidizes benzyl alcohol) driving a faster NHS^- oxidation. The oxidation of benzyl alcohol into
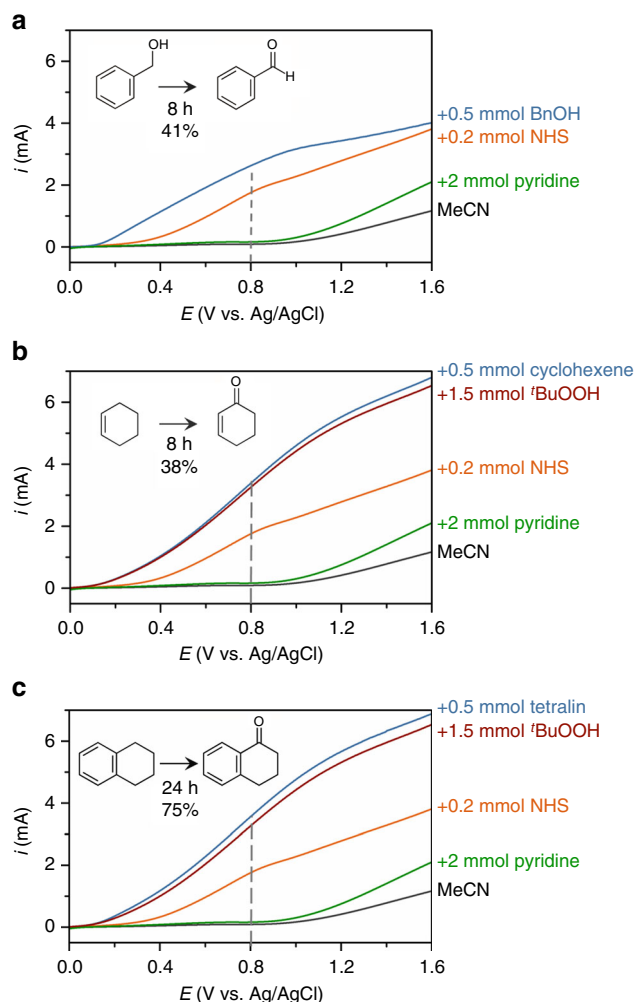

Fig. 3 LSV curves of PEC organic oxidation profiles. Photocurrents correspond to PEC oxidations of **a** benzyl alcohol to benzaldehyde, **b** cyclohexene to cyclohexanone, and **c** tetralin to 1-tetralone using a $BiVO_4$ photoanode immersed in 25 mL MeCN containing 0.1 M $LiClO_4$ and subjected to AM1.5 G light (scan rate = 10 mV s^{-1}). Photocurrent profiles correspond to the solvent and electrolyte solution (*black*) after the successive addition of 2 mmol pyridine (*green*), 0.2 mmol NHS (*orange*), 1.5 mmol of ^tBuOOH (*red*) and 0.5 mmol of the respective substrate (*blue*). The reaction yields determined by GC-MS are indicated. The *dashed line* indicates the $NHS^- \rightarrow NHS\bullet$ oxidation; this potential was used as the applied voltage, V_{app}, for PEC electrolysis experiments

benzaldehyde was confirmed by GC-MS, with a reaction yield of 41% after 8 h of PEC electrolysis (Supplementary Fig. 4). While further optimization is still needed to make the yield of benzaldehyde competitive with the best available synthetic methods, the result demonstrates the viability of performing PEC in a non-aqueous medium. These experiments also demonstrate that NHS can act as a useful redox mediator in tandem with a $BiVO_4$ photoanode.

Photoelectrochemical C-H oxidation. With evidence of a successful photoelectrochemical oxidation in non-aqueous media, we next explored the more synthetically challenging oxidation of cyclohexene to cyclohexanone (Fig. 3b) and tetralin to 1-tetralone (Fig. 3c). In addition to using NHS as a redox mediator, an external oxygen source, *tert*-butyl hydroperoxide (^tBuOOH), is used to form the requisite ^tBu peroxide-substrate adduct[26]. (Supplementary Fig. 8) Prior to addition of 0.5 mmol of substrate,
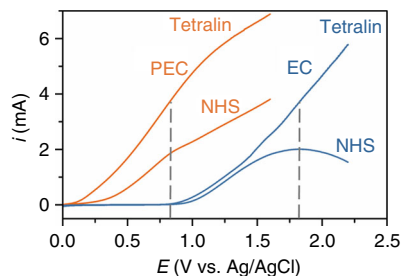
Fig. 4 Contrasting the photoelectrochemical and EC oxidation processes. The NHS-mediated oxidation of tetralin in a PEC cell (*orange*) is cathodically shifted by 1 V compared to an EC cell (EC; *blue*). The (photo)currents measured after adding pyridine and NHS to MeCN are denoted NHS, while the (photo)currents measured after adding ^tBuOOH and tetralin are denoted tetralin. The shoulder at 0.8 V and peak at 1.8 V (*dashed lines*) are attributed to the oxidation of NHS$^-$ to NHS$\bullet$ under PEC and EC conditions, respectively

3 equiv. of ^tBuOOH were shown to produce larger photocurrents than what was measured for pyridine, presumably due to the oxidation of ^tBuOOH. The PEC electrolysis experiments afforded cyclohexanone from cyclohexene (38% yield after 8 h, Supplementary Fig. 5) and 1-tetralone from tetralin (75% yield after 24 h; Supplementary Fig. 6a). The conversions were quantified by GC-MS to confirm 93% conversion of tetralin to 1-tetralone, which is corroborated with the coulombic charge passed through the PEC cell (Supplementary Figs. 6b and 7).

The PEC oxidations of each of the compounds appear to be mediated by NHS. In each of these schemes, a quasi-static equilibrium of photo-generated electron and hole populations leads to the separation of the BiVO$_4$ Fermi level (E_F) into quasi-Fermi levels for electrons ($E_{F,n}$) and holes ($E_{F,p}$)[3]. The difference between these two quasi-Fermi levels represents the photovoltage (V_{ph}), which serves to reduce the applied voltage (V_{app}) required to drive the reaction. The interfacial chemistry is then driven by the oxidation of deprotonated NHS to form NHS$\bullet$, which reacts with the substrate. (Control experiments ruled out a meaningful rate of oxidation without NHS; the replacement of NHS with *N*-methoxysuccinimide, which is not able to generate a radical, also did not show reactivity.) In the case of tetralin (a conjectured mechanism for tetralin photo-oxidation is provided in Supplementary Fig. 8), NHS$\bullet$ abstracts a hydrogen atom from tetralin to ostensibly form a stable benzylic radical species that ultimately leads to a peroxide intermediate that eliminates ^tBuOH to yield 1-tetralone. The reductive chemistry at the cathode is assumed to involve pyridinium. This proposal is in line with known chemistry[26], but experiments are underway to validate the proposed reaction steps and energetic profiles for each of these reactions.

Voltage reduction provided by PEC cell. We also quantified the electrical energy savings provided by AM1.5 G light for the oxidation of tetralin in the PEC cell vs. an EC cell with a glassy carbon electrode (Fig. 4). The oxidation of NHS$^-$ to NHS$\bullet$ was measured at 0.8 V and 1.8 V for the PEC and EC cell, respectively. These potentials each produced currents of ~3.8 mA and thus similar 75% yields of 1-tetralone after 24 h of (photo)electrolysis (Supplementary Fig. 7). This comparison indicates that illumination of the PEC cell enables V_{app} to be reduced by 1 V compared to that of the EC cell corresponding to a 60% reduction in energy savings.

The solar-to-electricity efficiency (η) of traditional PEC water oxidation can be calculated by the following relationship: $\eta = J^*(1.23\,V - V_{app})/P_{in}$, where J = photocurrent density, 1.23 V = E^o

(O_2/H_2O), V_{app} = applied potential in the PEC cell, and P_{in} = power density of illumination (100 mW cm^{-2} in this study). State-of-the-art BiVO$_4$ photoanodes that mediate PEC water oxidation at a V_{app} of 0.6 V generate $J = 2.73$ mA cm^{-2} and therefore yield $\eta = 1.7\%$. In our experiments in MeCN, the PEC cell was driven at 0.8 V to produce $J = 3.8$ mA/3 cm^2 = 1.3 mA cm^{-2}. Our EC cell required 1.8 V to yield the same J value of 1.3 mA cm^{-2}, and thus we assumed 1.8 V to effectively be the pseudo standard potential of NHS. Given that our illuminated photoanode area was 3 cm^2 and our light intensity was 100 mW cm^{-2}, the η of our cell is therefore 1.3%. This analysis shows that our PEC organic oxidation system offers higher-valued organic products at approximately the same energy efficiency as traditional PEC water oxidation.

In summary, we have demonstrated that illumination of BiVO$_4$ immersed in organic media drives both alcohol oxidation and C-H activation/oxidation. The use of light can reduce the applied voltage of an EC oxidation process by 1 V. The use of organic media in place of water affords markedly higher semiconductor photostability, thereby enabling sustained photochemical conversion over at least 1 day. This alternative PEC cell design highlights the potential to generate higher-value small molecules compared to traditional PEC cells.

Methods

Materials. Bismuth nitrate hexahydrate (98%), vanadyl acetylacetonate (98%), and tungsten hexachloride (99%) were purchased from Strem Chemicals and used as received. All other chemicals were purchased from commercial vendors (Acros Organics, Alfa Aesar, Fisher Scientific, or Sigma-Aldrich) and used as received. FTO substrates (TEC 15) were purchased from Hartford Glass Co. Glassy carbon electrodes were purchased from Alfa Aesar.

Electrode preparation. BiVO$_4$ photoanodes were prepared in accordance with previously reported procedures[10, 28]. Bismuth nitrate hexahydrate (0.346 g, 0.713 mmol), vanadyl acetylacetonate (0.176 g 0.663 mmol), and tungsten hexachloride (0.02 g, 0.05 mmol) were added to a 10 mL mixture of acetic acid and acetylacetone (1:8 v/v). The solution was sonicated for 15 min and then spin-coated onto a FTO substrate at 1000 rpm for 30 s. Each of the successive 16 coats was annealed at 500 °C for 10 min prior to a final 8 h annealing step at 500 °C. The BiVO$_4$ samples were irradiated with UV light (Model #: GPH436T5VH, Atlantic Ultraviolet Co.; $\lambda_{max} \sim 254$ nm and 185 nm; flux ~10 mW cm^{-2} at 5.5 cm in our experiment) for 20 h. The geometric surface areas of all working electrodes (BiVO$_4$ photoanodes and glassy carbon electrodes) in this study were 3 cm^2.

Photoelectrochemical and electrochemical oxidation. PEC and EC electrolysis were performed with a CHI 660D potentiostat in a three-electrode photoelectrochemical cell with a BiVO$_4$ photoanode (for PEC experiments) or glassy carbon (electrochemistry experiments) as the working electrode, Ag/AgCl as the RE, and glassy carbon as the CE. PEC measurements and electrolysis were conducted under AM1.5 G simulated sunlight with an Oriel 94011A-ES solar simulator integrated with a 100-W xenon arc lamp and AM1.5 G filter. An infrared water filter was applied to prevent the solution from heating up during PEC electrolysis. Experiments were performed in 0.1M LiClO$_4$ in 25 mL MeCN or 0.1M NaHCO$_3$ in H$_2$O (buffered to pH 7). Potentials were measured vs. Ag/AgCl, which was calibrated to 0.196 V vs. NHE in aqueous media. For the dark and photocurrent measurements, LSV was measured prior to performing electrolysis, and the scan rate was maintained at 10 mV s^{-1}. For PEC and EC oxidations of organic substrates: pyridine (2 mmol, 4 equiv.), NHS (0.2 mmol, 40 mol%), ^tBuOOH (70% in H$_2$O, 1.5 mmol, 3 equiv. for cyclohexene and tetralin oxidations) and substrate (0.5 mmol, 1 equiv.) were added successively to a 0.1M LiClO$_4$ solution in 25 mL MeCN. Control experiments were performed under the same condition, except that each of the said reagents was added in exclusivity. PEC/EC electrolysis was performed at room temperature, using a constant potential method (0.8 V and 1.8 V vs. Ag/AgCl for PEC and EC electrolysis, respectively) with magnetic stirring.

Gas chromatography-mass spectrometry. Samples were taken during and after electrolysis and carvone was added as an internal standard. GC-MS measurements were run on an Agilent GC-MS instrument with a HP-5ms GC column and electron ionization ion source. A 1-μL aliquot was injected with an auto-sampler using split mode with a split ratio of 20:1, and carried by He gas at a flow rate of 1 mL min^{-1}. The oven temperature started at 60 °C for 1 min, then ramped from 100 to 150 °C at 20 °C min^{-1} and from 150 to 250 °C at 40 °C min^{-1}. Detection was not performed for the first 1.75 min of the run, or the solvent delay time. GC-MS

peaks were identified using the NIST Mass Spectrometry Data Center database (all peak identifications exhibited a probability match of >90%) and compared with peaks in standard solutions. For quantitative analysis, a series of standard solutions with known concentrations of reactants and products were prepared and carvone was added as an internal standard. Standard solutions were run by GC-MS using the same method, and the relative peak areas of reactants and products were normalized to the internal standard peak. Linear calibration curves were plotted to quantify the concentrations of reactants and products.

Physical methods. Absorptivity measurements of $BiVO_4$ samples were collected with a PerkinElmer Lambda 35 UV-Vis spectrometer with a solid sample holder accessory. Baseline scans were recorded on clean FTO. X-ray diffraction characterization was conducted using a Bruker F8 Focus X-ray diffractometer. Data were collected between 2θ angles of 5° and 90° with a step size of 0.04° and the step time was 0.6 s. Film morphologies were investigated using a Helios NanoLab 650 Focused Ion Beam SEM, with the accelerating voltage kept at 1 kV and the current at 50 pA for imaging.

Data availability. The authors declare that the main data supporting the findings of this study are available within the article and its Supplementary Information files. Extra data are available from the corresponding author upon request.

References

1. Grätzel, M. Photoelectrochemical cells. *Nature* **414**, 338–344 (2001).
2. Lewis, N. S. & Nocera, D. G. Powering the planet: chemical challenges in solar energy utilization. *Proc. Natl Acad. Sci. USA* **103**, 15729–15735 (2006).
3. Walter, M. G. et al. Solar water splitting cells. *Chem. Rev.* **110**, 6446–6473 (2010).
4. Sivula, K. Metal oxide photoelectrodes for solar fuel production, surface traps, and catalysis. *J. Phys. Chem. Lett.* **4**, 1624–1633 (2013).
5. Hu, K. et al. Kinetic pathway for interfacial electron transfer from a semiconductor to a molecule. *Nat. Chem.* **8**, 853–859 (2016).
6. Cox, C. R., Winkler, M. T., Pijpers, J. J. H., Buonassisi, T. & Nocera, D. G. Interfaces between water splitting catalysts and buried silicon junctions. *Energy Environ. Sci.* **6**, 532–538 (2013).
7. Du, C. et al. Hematite-based water splitting with low turn-on voltages. *Angew. Chem. Int. Ed.* **52**, 12692–12695 (2013).
8. Kim, T. W. & Choi, K.-S. Nanoporous $BiVO_4$ photoanodes with dual-layer oxygen evolution catalysts for solar water splitting. *Science* **343**, 990–994 (2014).
9. Li, T., He, J., Peña, B. & Berlinguette, C. P. Exposure of WO_3 photoanodes to ultraviolet light enhances photoelectrochemical water oxidation. *ACS Appl. Mater. Interfaces* **8**, 25010–25013 (2016).
10. Zhong, D. K., Choi, S. & Gamelin, D. R. Near-complete suppression of surface recombination in solar photoelectrolysis by 'Co-Pi' catalyst-modified W:$BiVO_4$. *J. Am. Chem. Soc.* **133**, 18370–18377 (2011).
11. Zhong, M. et al. Surface modification of CoO_x loaded $BiVO_4$ photoanodes with ultrathin p-Type NiO layers for improved solar water oxidation. *J. Am. Chem. Soc.* **137**, 5053–5060 (2015).
12. Cha, H. G. & Choi, K.-S. Combined biomass valorization and hydrogen production in a photoelectrochemical cell. *Nat. Chem.* **7**, 328–333 (2015).
13. Ager, J. W., Shaner, M. R., Walczak, K. A., Sharp, I. D. & Ardo, S. Experimental demonstrations of spontaneous, solar-driven photoelectrochemical water splitting. *Energy Environ. Sci.* **8**, 2811–2824 (2015).
14. Seabold, J. A. & Choi, K.-S. Effect of a cobalt-based oxygen evolution catalyst on the stability and the selectivity of photo-oxidation reactions of a WO_3 photoanode. *Chem. Mater.* **23**, 1105–1112 (2011).
15. Jia, Q., Iwashina, K. & Kudo, A. Facile fabrication of an efficient $BiVO_4$ thin film electrode for water splitting under visible light irradiation. *Proc. Natl Acad. Sci. USA* **109**, 11564–11569 (2012).
16. Kim, T. W. & Choi, K.-S. Improving stability and photoelectrochemical performance of $BiVO_4$ photoanodes in basic media by adding a $ZnFe_2O_4$ Layer. *J. Phys. Chem. Lett.* **7**, 447–451 (2016).
17. Vuyyuru, K. R. & Strasser, P. Oxidation of biomass derived 5-hydroxymethylfurfural using heterogeneous and electrochemical catalysis. *Catal. Today* **195**, 144–154 (2012).
18. Tojo, G. & Fernandez, M. I. *Oxidation of Alcohols to Aldehydes and Ketones*. (Springer Science & Business Media, 2006).
19. Bäckvall, J.-E. *Modern Oxidation Methods*. (John Wiley & Sons, 2011).
20. You, B., Liu, X., Jiang, N. & Sun, Y. A general strategy for decoupled hydrogen production from water splitting by integrating oxidative biomass valorization. *J. Am. Chem. Soc.* **138**, 13639–13646 (2016).
21. Badalyan, A. & Stahl, S. S. Cooperative electrocatalytic alcohol oxidation with electron-proton-transfer mediators. *Nature* **535**, 406–410 (2016).
22. Hickey, D. P. et al. Predicting electrocatalytic properties: modeling structure–activity relationships of nitroxyl radicals. *J. Am. Chem. Soc.* **137**, 16179–16186 (2015).
23. Song, W. et al. Visible light driven benzyl alcohol dehydrogenation in a dye-sensitized photoelectrosynthesis cell. *J. Am. Chem. Soc.* **136**, 9773–9779 (2014).
24. Weidmann, V. & Maison, W. Allylic oxidations of olefins to enones. *Synthesis* **45**, 2201–2221 (2013).
25. Trost, B. M., Semmelhack, M. F. & Fleming, I. *Comprehensive Organic Synthesis*. (Elsevier, 1991).
26. Horn, E. J. et al. Scalable and sustainable electrochemical allylic C-H oxidation. *Nature* **533**, 77–81 (2016).
27. Shono, T. & Ikeda, A. Electroorganic chemistry X anodic allylic substitution. *J. Am. Chem. Soc.* **94**, 7892–7898 (1972).
28. Li, T., He, J., Peña, B. & Berlinguette, C. P. Curing $BiVO_4$ photoanodes with ultraviolet light enhances photoelectrocatalysis. *Angew. Chem. Int. Ed.* **55**, 1769–1772 (2016).
29. Trześniewski, B. J. & Smith, W. A. Photocharged $BiVO_4$ photoanodes for improved solar water splitting. *J. Mater. Chem. A* **4**, 2919–2926 (2016).
30. Navaee, A. & Salimi, A. N-hydroxysuccinimide-mediated photoelectrooxidation of aliphatic alcohols based on cadmium telluride nanoparticles decorated graphene nanosheets. *Electrochim. Acta* **105**, 230–238 (2013).

Acknowledgements

Author contributions

C.P.B. and G.M.S. supervised this project; T.L., T.K., G.M.S., and C.P.B. designed the experiments; T.L. performed the PEC oxidations and GC-MS analysis, T.K. performed preliminary experiments, J.H. performed the EC oxidation and K.E.D. obtained SEM images; T.L., T.K., G.M.S., and C.P.B. wrote the manuscript.

Additional information

Supplementary Information accompanies this paper at doi:10.1038/s41467-017-00420-y.

Competing interests: The authors declare no competing financial interests.

Reprints and permission information is available online at http://npg.nature.com/reprintsandpermissions/

Publisher's note: Springer Nature remains neutral with regard to jurisdictional claims in published maps and institutional affiliations.